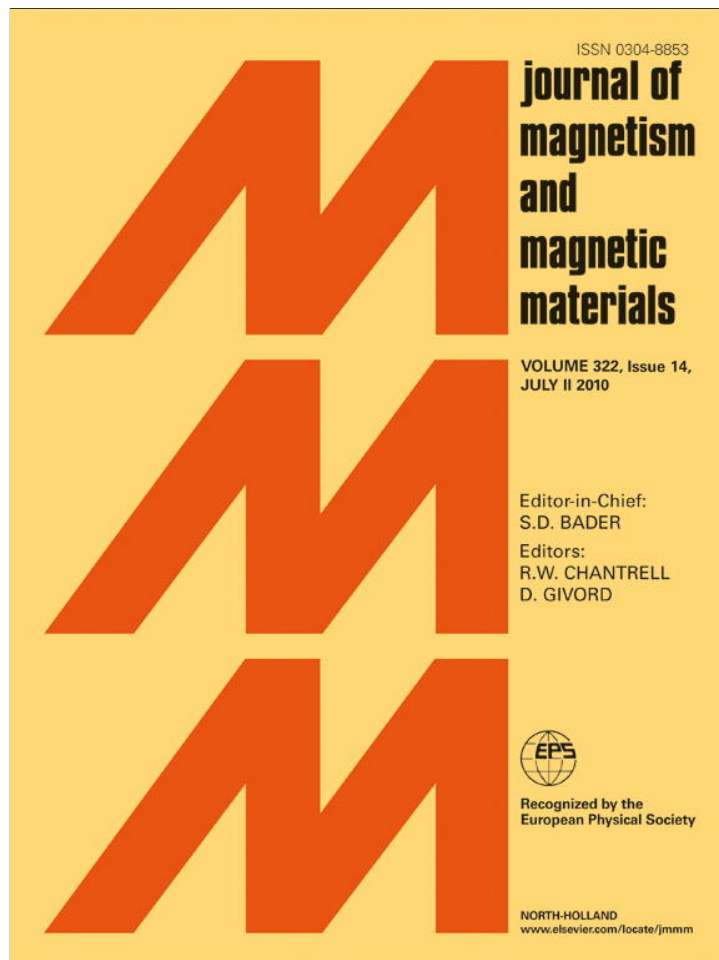


Provided for non-commercial research and education use.  
Not for reproduction, distribution or commercial use.



This article appeared in a journal published by Elsevier. The attached copy is furnished to the author for internal non-commercial research and education use, including for instruction at the authors institution and sharing with colleagues.

Other uses, including reproduction and distribution, or selling or licensing copies, or posting to personal, institutional or third party websites are prohibited.

In most cases authors are permitted to post their version of the article (e.g. in Word or Tex form) to their personal website or institutional repository. Authors requiring further information regarding Elsevier's archiving and manuscript policies are encouraged to visit:

<http://www.elsevier.com/copyright>



Contents lists available at ScienceDirect

## Journal of Magnetism and Magnetic Materials

journal homepage: [www.elsevier.com/locate/jmmm](http://www.elsevier.com/locate/jmmm)

## Magnetic properties of ErN films

C. Meyer<sup>a,b,\*</sup>, B.J. Ruck<sup>a</sup>, A.R.H. Preston<sup>a</sup>, S. Granville<sup>a</sup>, G.V.M. Williams<sup>c</sup>, H.J. Trodahl<sup>a</sup><sup>a</sup> The MacDiarmid Institute for Advanced Materials and Nanotechnology, School of Chemical and Physical Sciences, Victoria University, PO Box 600, Wellington 6140, New Zealand<sup>b</sup> Institut Néel (CNRS and UJF), 25 rue des Martyrs, BP 166, F-38042 Grenoble, France<sup>c</sup> The MacDiarmid Institute for Advanced Materials and Nanotechnology, Industrial Research Ltd., PO Box 31310, Lower Hutt 5040, New Zealand

## ARTICLE INFO

## Article history:

Received 3 September 2009

Available online 18 January 2010

## Keywords:

Thin film  
Nitride  
Evaporation  
Ultra high vacuum  
Erbium  
ErN  
Resistivity  
Magnetic structure  
Magnetic anisotropy  
Crystal field  
Nanocrystalline

## ABSTRACT

We report a magnetization study of stoichiometric ErN nanocrystalline films grown on Si and protected by a GaN passivating layer. According to the temperature dependence of the resistivity the films are heavily doped semiconductors. Above 100 K the magnetization data fit well to a Curie–Weiss behavior with a moment expected within the free-ion  $\text{Er}^{3+}$   $J = \frac{15}{2}$  multiplet. Below 50 K the Curie–Weiss plot steepens to an effective moment corresponding to that in the crystal-field determined quartet ground state, and develops a clear paramagnetic Curie–Weiss temperature of about 4.5 K. Zero-field- and field-cooled magnetization curves and the AC susceptibility firmly establish a ferromagnetic ground state within that multiplet below a Curie temperature of  $6.3 \pm 0.7$  K. Due to the (1 1 1) texture of the film the comparison between the magnetization behavior, when the field is applied parallel and perpendicular to the film plane, gives new information about the magnetic structure. An arrangement of the moments according to the model derived from neutron diffraction for bulk HoN is strongly suggested.

© 2010 Elsevier B.V. All rights reserved.

## 1. Introduction

Although examined in the 1960s, the magnetic properties of the rare earth mononitrides (RN) have since been largely ignored, with the exception of GdN, until a recent resurgence of interest [1]. Perhaps the strongest driving factor for the revival is that improvements in the band calculations for strongly correlated electrons have permitted their electronic structure to be better described. Within the series there are now predictions of ferromagnetic semiconductors and half metals [2], both of which might be of interest for spintronics applications. However, there are experimental challenges to a study of these nitrides, which are difficult to prepare oxygen-free and stoichiometric, and until recent advances there remained uncertainty about whether their ground states are metallic or semiconducting. Using a parallel development of experimental and theoretical work, we have recently shown that GdN is a small gap semiconductor with potentially spin polarized carriers [3,4]. Subsequently, we have found that DyN and SmN are also ferromagnetic semiconductors in their ground states [5,6]. In the present paper we describe the

magnetic properties of ErN films. The results are discussed in the light of recent theoretical predictions of the band structure [7].

Er has eleven  $4f$  electrons leading for  $\text{Er}^{3+}$  to a well-isolated ground state  $J = \frac{15}{2}$  and a free ion magnetic moment  $m_0 = g_J \mu_B = 9 \mu_B$  (with the Landé factor  $g_J = 6/5$ ). Earlier magnetic data on bulk ErN are collected in the reviews of RE pnictides [1,8,9]. Those data all agree that ErN is ferromagnetic, but with Curie temperatures that vary between 3.4 and 6 K. There is a rough agreement about the paramagnetic state: in the high temperature range ( $T \leq 750$  K) where the crystal field splitting is smaller than  $k_B T$ , the susceptibility follows a Curie–Weiss law with a magnetic moment of  $9.4 \mu_B (\pm 0.1)$  close to the free ion  $\text{Er}^{3+}$  value,  $m_{\text{eff}}(T) = g_J \sqrt{J(J+1)} \mu_B = 9.59 \mu_B$ . The paramagnetic Curie temperature  $\theta_p$  varies from +4 K [10,11] to +14 K [12]. The spontaneous moment of  $5.5 \mu_B$  in the ferromagnetic state is lower than  $m_0$ , which has been attributed to an exchange interaction that is smaller in comparison to the crystal field splitting. Thus, saturation is not yet achieved under an applied field of 13 T ( $7.9 \mu_B$ ) [10,11]. Neutron diffraction experiments also reported a ferromagnetic ordering, characterized for HoN and ErN by a complicated non-collinear magnetic structure with successive ferromagnetic sheets perpendicular to [111] [13]. For ErN a magnetic moment of  $6 \mu_B/\text{ion}$  was reported and the reduction with respect to the free ion moment attributed to the crystal field effect. A more detailed analysis of HoN suggested a retarded spiral structure with the moments along the  $\langle 100 \rangle$  directions giving

\* Corresponding author at: Institut Néel (CNRS and UJF), 25 rue des Martyrs, BP 166, F-38042 Grenoble, France.

E-mail addresses: [claire.meyer@grenoble.cnrs.fr](mailto:claire.meyer@grenoble.cnrs.fr) (C. Meyer), [ben.ruck@vuw.ac.nz](mailto:ben.ruck@vuw.ac.nz) (B.J. Ruck).

rise to a net ferromagnetic moment along [1 1 1]. As pointed out by Vogt and Mattenberger [9,14], such a spin arrangement in a modern view would be rather described as a multi-Q structure, with a coexistence of antiferro- and ferromagnetic ordered components of the spins.

In contrast to the magnetism, authors have shown no consistent view of the electronic properties of ErN samples. The first experimental data obtained on ErN evidenced the complexity of the problem due to a lack of stoichiometry. Early reports [15] suggest an optical gap near 2 eV, together with a resistivity of the order of  $100 \mu\Omega\text{cm}$  at room temperature, which shows a metallic behavior with a large concentration of electron carriers, attributed to nitrogen vacancies. This behavior was in fact found for most of the RN in those early studies.

There is no consensus about the computed band structure of ErN. According to successive band calculations in a local-spin-density approximation (LSDA), ErN was first found to be metallic through a LSD plus self-interaction corrections (SIC) method [2], and then semiconducting within the LSDA+U approach, for which a small 0.2 eV indirect gap is predicted [7]. However, another LSDA+U calculation found [1] a half-metallic zero-gap in ErN. A half metallic ground state has also been obtained in a spin polarized charge-self-consistent density functional based tight binding (DFTB) approach [16]. Both the electronic structure and magnetic ordering have been investigated theoretically in ErAs and ErN [17]. An antiferromagnetic ordering was predicted for both compounds in agreement with the experiment for ErAs but not for ErN. The authors suggested the dipolar interaction might take part in the magnetic ordering and also explain the magnetic anisotropy. As a matter of fact, according to Trammell [18], the minimum in the dipolar energy occurs when the moments are perpendicular to the [1 1 1] direction. Note that magneto-transport studies suggest that the dipole–dipole interactions are the dominant exchange mechanism in ErAs [19].

It is interesting that ErN was also recently reinvestigated for its huge magneto-caloric effect, which makes it a potential material for magnetic refrigeration at helium temperature [20]. Arrott plots of the magnetization curves provide a Curie temperature  $T_C = 8 \pm 2$  K. The specific heat exhibits a  $\lambda$ -type anomaly peak at 4.4 K.

The aim of the present work is to re-examine the properties of ErN using films that have been shown to display a high stoichiometry compared to the aforementioned bulk samples. We find that ErN is a highly doped ferromagnetic semiconductor and we show that the magnetic behavior in the ordered state is well explained assuming an exchange field much smaller than the crystal field splitting derived from a simple point charge model.

## 2. Film preparation and characterization

The films were grown by thermal evaporation in an ultra-high vacuum chamber as described previously [3]. Er metal was evaporated in the presence of  $10^{-4}$  mbar of ultra-high purity  $N_2$  gas and deposited on a Si(111) substrate held at room temperature. The native oxide upon the Si surface was not removed so that ErN grows on an amorphous oxide layer. A capping layer of GaN was deposited to protect against oxidation in the outer atmosphere. The resistance was measured *in situ* and monitored as the system was vented to determine that the capping layer was effective. The thickness and composition were measured by Rutherford backscattering spectroscopy (RBS) and nuclear reaction analysis (NRA). The configuration of the ErN thin film investigated in the present work is Si(400  $\mu\text{m}$ )/ErN(215 nm)/GaN(90 nm). The composition of the film showed

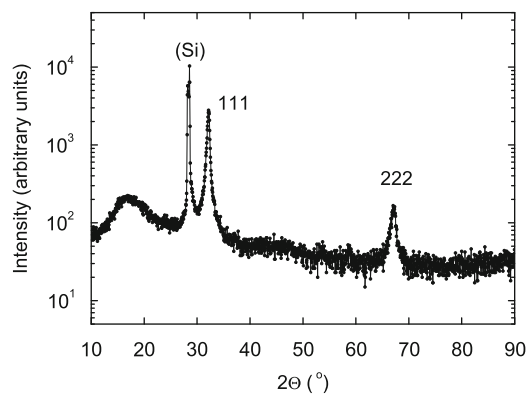


Fig. 1. X-ray diffraction diagram of the ErN film ( $\lambda_{\text{Cu}}$ ).

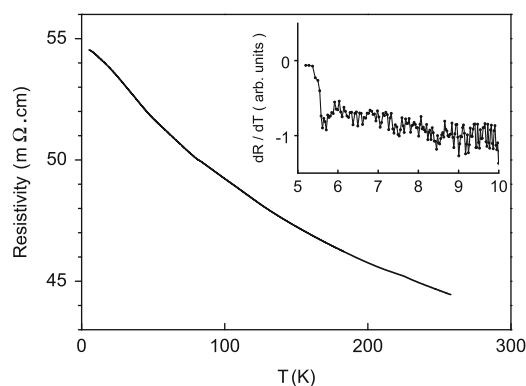


Fig. 2. Temperature dependence of the resistivity. Inset: derivative of the resistivity showing an upturn below 6 K.

the expected 1:1 stoichiometry for ErN (within a 1% error). Not more than 1–2% oxygen was found in the film.

Fig. 1 shows the X-ray diffraction pattern obtained for the film with the Cu  $K\alpha$  radiation. A strong (1 1 1) texture develops during growth onto the amorphous  $\text{SiO}_x$  surface layer. The line broadening reflects a coherence length of the crystallites of 20 nm in the direction perpendicular to the film. Compared to the characteristic length scale of magnetism, this size is larger than the exchange length ( $\approx 6$  nm) or the Bloch domain wall width ( $\approx 15$  nm) so that bulk-like magnetic behavior is expected, together with the 2D shape effect associated with the thin film geometry. A random in-plane orientation of the crystallites is assumed with respect to their [1 1 1] axis. The lattice parameter of the NaCl face-centered-cubic structure was derived to be  $4.836 \pm 0.005 \text{ \AA}$ , comparable to the literature bulk data of  $4.83 \text{ \AA}$ . As oxygen inclusions in RN have been demonstrated to decrease the lattice parameter [21,22], we believe that the ErN film is highly stoichiometric and that potential residual oxygen is confined at the interface.

The DC electrical resistivity was measured *ex situ* as a function of the temperature between 300 and 5.2 K, shown in Fig. 2. The relatively small negative temperature coefficient and the room temperature resistivity of  $0.04 \Omega\text{cm}$  are both characteristic of a heavily doped semiconductor, similar to our results on previously grown RN films [3,5,23]. Recalling that the stoichiometry determination is accurate to 1% at best, we believe that N vacancies dope the film, as has been demonstrated to be the case in GdN films grown by the same process [3]. A clear upturn occurs at the Curie temperature (see next section) when the derivative of the resistivity is plotted, as can be seen in the inset of Fig. 2. This phenomena is observed in other RN films [5].

### 3. Magnetic measurements

Magnetization measurements were performed with a SQUID magnetometer with a maximum field of 6T applied mainly parallel to the film plane. Some complementary experiments were carried out in the perpendicular geometry. The diamagnetic contribution from the Si substrate is small in comparison to the magnetic signal of the RN but cannot be neglected. Measurements of a bare substrate show a susceptibility of  $-3.3 \times 10^{-6} \pm 10\%$ , close to the theoretical Si susceptibility  $\chi(\text{Si}) = -3.4 \times 10^{-6}$  at 300K.

Magnetization isotherms were measured at 16 temperatures between 2 and 300 K, and a selection are represented in Fig. 3. The isotherms are linear with the applied field for temperatures down to 50K, compatible with a Curie–Weiss behavior. Below 50K the magnetization is curved according to a Brillouin evolution at high field and the probable influence of the crystal field. The susceptibility at zero-field increases sharply below 10K and a close look at low field shows the presence of a hysteresis loop in the temperature range 2–5K, as reproduced for 2K in Fig. 4. The critical field is about 0.2T with a coercive field of 20 mT and there is a very small remanent magnetization of  $0.2\mu_B/\text{Er}^{3+}$ . The occurrence of a ferromagnetic ordering is accompanied by a non-saturation of the magnetization at high field, as has been reported previously [10,11]. At 2K, the magnetization in 6T is only  $5\mu_B/\text{Er}^{3+}$ . The linear behavior found in the magnetically ordered region is attributed to the rotation of the magnetic moments from their easy direction towards the applied field direction, as a large magnetocrystalline anisotropy is expected for  $\text{Er}^{3+}$  compounds. Moreover, a non-collinear arrangement of the moments has been suggested by neutron experiments as discussed above. This magnetic structure would also explain the small remanence. Extrapolation to the origin of the high field pseudo-linear contribution provides an order of magnitude of the spontaneous magnetic moment  $\mu_{\text{extr}} = 3.85 \pm 0.05\mu_B$  at 2K. In fact if we refer to the magnetic structure proposed for HoN [13], this value rather corresponds to the virtual arrangement of the moments parallel to the randomly distributed  $\langle 100 \rangle$  directions along two half-cones of axis  $[111]$  and angle  $54.73^\circ$ . The average of the spontaneous magnetization is therefore  $\pi/(2\sqrt{6})M_s$ , leading to  $M_s = 6 \pm 0.1\mu_B$ , in perfect agreement with neutron diffraction.

To improve our knowledge of the magnetic structure and of the anisotropy energy, we have performed magnetization measurements in the perpendicular geometry i.e. with the magnetic field applied perpendicular to the film plane and parallel to the  $[111]$  axis. Some curves are shown in Fig. 5. They exhibit the same ferromagnetic behavior below 10K, apart from the

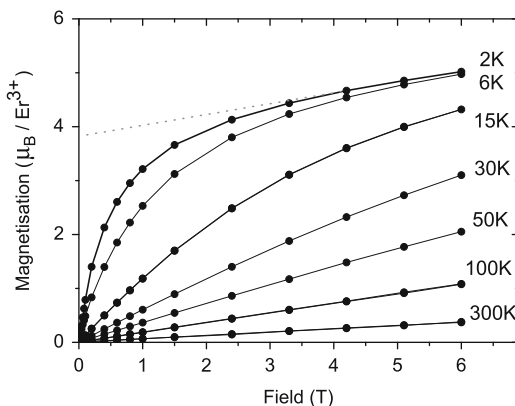


Fig. 3. In-plane magnetization isotherms.

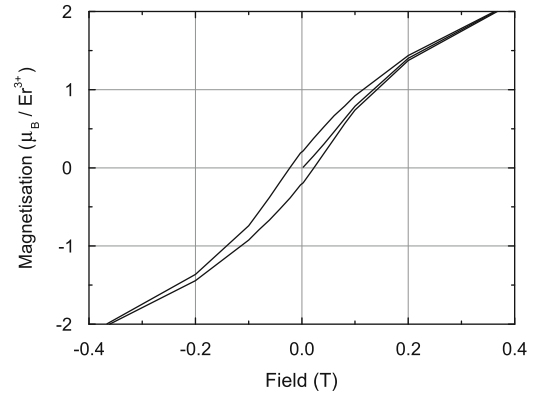


Fig. 4. Detail of the hysteresis loop observed at  $T = 2\text{K}$ .

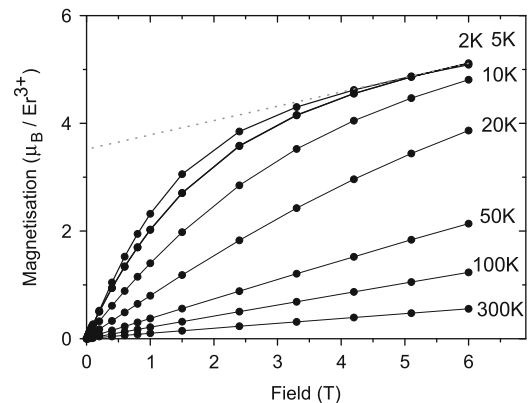
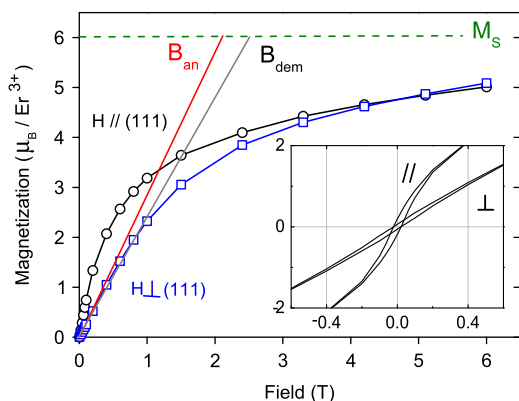


Fig. 5. Magnetization isotherms with the magnetic field applied perpendicular to the film plane.

demagnetizing field effect. An extrapolation of the high field part of the 2K curve crosses the  $M$  axis at  $M_{\text{perp}} = 3.53 \pm 0.06\mu_B$ . In that case we assume that the magnetization lies randomly oriented on the full cone of angle  $54.73^\circ$  centered on the applied field direction  $[111]$ . The virtual residual magnetization is  $(1/\sqrt{3})M_s$  and thus  $M_s = 6.1 \pm 0.1\mu_B$ , which is again consistent with the parallel value.

The review paper of Vogt and Mattenberger [9] has proposed an easy moment direction perpendicular to  $[111]$ , in direct disagreement with the HoN-like spiral magnetic structure involving a  $[001]$  easy-axis within which we have interpreted our data. However, the question is still open, for there are no data in the literature that directly support the  $[111]$ -perpendicular easy axis direction. We now demonstrate that our data cannot be interpreted within that model. In that picture the present film magnetization should lie in-plane parallel to a high symmetry axis like  $\langle 110 \rangle$ , with no perpendicular component of the magnetization. The spontaneous magnetization in-plane should be  $0.5M_s$  giving rise to  $M_s = 7.7 \pm 0.1\mu_B$ . The spontaneous magnetization perpendicular to the plane should correspond to the magnetic moments randomly distributed along the  $\langle 110 \rangle$  directions defining a cone of axis  $[111]$  and angle  $35.26^\circ$ , therefore  $0.81M_s$  giving rise to  $M_s = 4.3 \pm 0.1\mu_B$ . In that case there is no agreement between the two geometries.

In Fig. 6 the magnetization curves at 2K along the two directions are compared. The area between the curves is proportional to the anisotropy energy difference mainly due the demagnetizing field energy at low field. The contribution of the erbium magnetocrystalline energy is an order of magnitude higher if we refer to the anisotropy constant in rare earth metals ( $10^7 \text{J/m}^3$ ). There is a small aperture in the perpendicular loop,



**Fig. 6.** (Color online) First magnetization at 2K with the magnetic field applied parallel (circles) and perpendicular (squares) to the film plane (111). Inset: hysteresis loop in the two configurations.

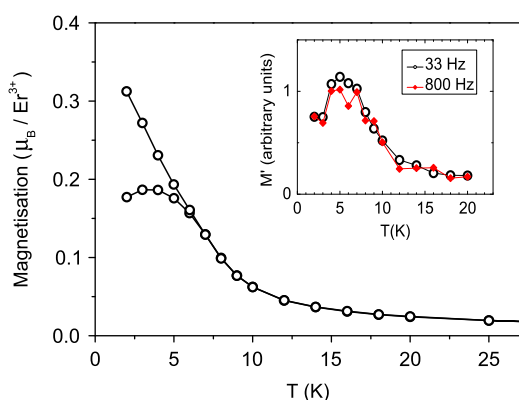


**Fig. 7.** (Color online) Magnetization versus  $T$  in an in-plane applied field of 25 mT in the low temperature region where a hysteresis takes place in a ZFC-FC measurement process. The inset shows the AC-susceptibility measured at two different frequencies in zero applied DC-field.

shown in the inset of the figure. This irreversibility suggests the existence of domains not strictly parallel to the film plane, which is expected if the arrangement of the moments is non collinear. The zero-field susceptibility should give nearly the demagnetizing field slope. The anisotropy field is determined as the crossing point with the saturation magnetization:  $\mu_0 H_{an} = 2.1$  T. The theoretical demagnetizing field calculated for  $M_s = 6\mu_B$  is  $\mu_0 H_{dem} = 2.48$  T. Even if the difference is not very large, it is probably real. This would mean that the energy necessary to overcome the film shape effect is less than the magnetostatic energy and this is consistent with a non-zero component of the magnetization perpendicular to the film plane, once again in agreement with the non-collinear magnetic structure described from neutron diffraction in HoN.

The temperature dependence of the in-plane magnetization at low field (25 mT) shows a clear upturn at low temperature and the magnetization becomes irreversible below about 6.5 K, as indicated by the zero field cooled/field cooled (ZFC/FC) data shown in Fig. 7. Thus, below 6 K the applied field used for these measurements is smaller than the coercive field, as already seen in the hysteresis loops. A field of 25 mT is not sufficient to induce the reversal of the inverse domains in the demagnetized sample. The maximum of the derivative of the FC curve occurs at  $T = 7$  K, providing the first estimate of the Curie point in this film.

We have also measured the AC-susceptibility in zero applied field at low temperature and two frequencies, 33 and 800 Hz, for the 0.2 mT AC-field (inset of Fig. 7). A maximum of the curves at

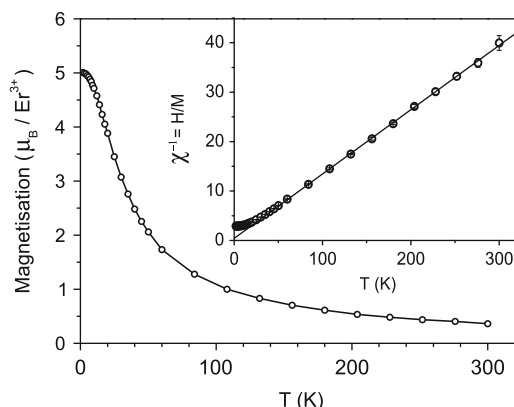


**Fig. 8.** Magnetization in the maximum field of 6T applied in-plane. Inset: plot of  $H/M$  in 6T. The solid line is a Curie-Weiss fit in the 100–300 K temperature range.

$T = 5.5 \pm 1$  K provides another estimate of the onset of the magnetic transition. Note that the anomaly in the thermal variation of the resistivity also takes place at this temperature. Consequently, we infer the average Curie point of ErN to be  $T_C = 6.3 \pm 0.7$  K.

The temperature dependence of the in-plane magnetization under the maximum field of 6T is plotted in Fig. 8. The magnetization shows a tendency to saturation at low temperature as expected in a ferromagnet. To analyze quantitatively the temperature dependence of the magnetization in the paramagnetic state, we have focused on the temperature range where the moment is linear as a function of the applied field ( $T = 100$ –300 K) and set  $\chi(T) = M(T)/H$  (see Fig. 3). The reciprocal susceptibility  $\chi^{-1}(T)$  is plotted in Fig. 8.

The curve is linear above  $T = 50$  K. A Curie-Weiss fit of  $\chi^{-1} = (T - \theta_p)/C$ , within the range 100–300 K, provides  $\mu_{eff} = 9.11 \pm 0.07\mu_B$  and  $\theta_p = -3 \pm 2.5$  K. However, the quantitative analysis of the susceptibility at high temperature depends on the correction arising from the Si substrate. For example if we use the theoretical Si susceptibility, we rather find:  $\mu_{eff} = 8.74 \pm 0.07\mu_B$  and  $\theta_p = +3.8 \pm 2.5$  K. On average, we end up with  $\mu_{eff} = 9.0 \pm 0.3\mu_B$  and  $\theta_p = 0 \pm 4$  K. These uncertainties arise from the limited fitting range in the high temperature region, which we cannot extend above room temperature as in previous studies. Nevertheless we obtain the magnitude of the effective moment close to the free ion value of  $9.59\mu_B$ , in agreement with the earlier data.

We can get more detailed information by focusing on low-temperature data. The very low magnetic ordering temperature implies that the exchange field interaction is much smaller than the crystal field splitting, which is generally of the order of several 100 K in the RN [8]. Therefore, the magnetic ordering does not involve the full multiplet as excited at temperatures above  $T = 50$  K, but takes place in the low-lying crystal field sublevel. To investigate the susceptibility at lower temperature it is necessary to investigate only the low-field data, which are unaffected by saturation associated with the Brillouin function. We thus plot in Fig. 9 the inverse of the initial slope of the magnetization isotherms as a function of temperature. Note that these data have been corrected assuming the measured value of the substrate susceptibility, though at this low field that correction is very small and Fig. 9 is entirely unaffected by using instead the alternative value discussed above. The points above  $T = 50$  K are superimposed on the 6 T ( $H/M$ ) curve as expected, but there is a strong deviation at lower temperature. Below  $T = 50$  K the low-field curve falls below the 6 T data, and at

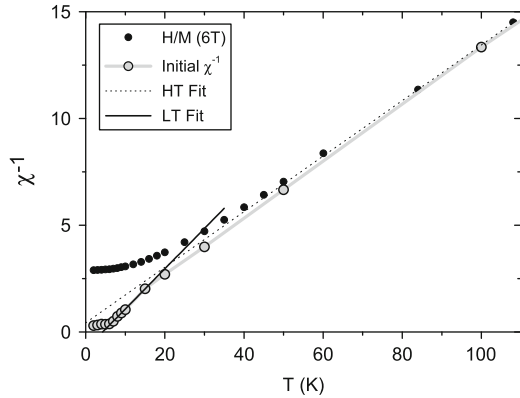


**Fig. 9.** Plot of the inverse of the initial slope of the parallel isotherms (open circles) as a function of  $T$ . The black circles are  $(H/M)$  in an applied field of 6 T. The Curie-Weiss fit in the high temperature regime is represented as a dotted curve and the full line curve is the fit in the low temperature regime of the linear part of the initial slope.

$T = 20$  K it shows a change in slope, followed by saturation below the Curie temperature of 6 K. A fit of the linear portion below the inflection point (approximately between  $T=7$  and 15 K) gives  $\mu_{\text{eff}} = 7.56 \pm 0.1 \mu_B$  and  $\theta_p = 4.3 \pm 0.4$  K. These data thus imply a ferromagnetic exchange interaction, with a reduced moment on the Er ions when in the ground state of the crystal field split multiplet.

The crystal field splitting level scheme is unknown for ErN, so any calculation has to make use of an approximate set of most probable data. In the review by Hulliger [8] the crystal field calculation performed by the authors in the approximation of a point charge model gives a quartet ground state level  $\Gamma_8^{(1)}$ , separated from the excited levels  $\Gamma_8^{(2)}$  and  $\Gamma_7$  by about 70 K in the purely ionic assumption, while the full crystal field splitting is  $E/k_B = 340$  K. To get some more information, we can refer to the crystal field level configuration experimentally derived for ErAs in an ErAs/GaAs epitaxial film, from infrared spectroscopy [24]. The ground state  $\Gamma_8^{(1)}$  quartet is separated from the first excited states,  $\Gamma_8^{(2)}$  and  $\Gamma_7$  by an energy of  $27.2 \text{ cm}^{-1}$  (39 K). This experimental result is in reasonable agreement with the point charge model approximation, in which this difference of energy is calculated as  $\Delta E = 10.5Z$  K, where  $Z$  is the effective ligand charge around  $\text{Er}^{3+}$ . For ErN within the same point charge model approximation  $\Delta E = 23.8Z$  K, [8] and assuming the same  $Z$ , we derive  $\Delta E = 91$  K. However, in the RN, the effective parameter  $Z$  is found to be larger than in the other rare earth pnictides [8]. Therefore, this value of  $\Delta E$  might be even larger. If we take  $Z = 3$ , in the purely ionic model, we get  $\Delta E = 71$  K. So it is reasonable to assume  $\Delta E = 90 \pm 20$  K. This is large compared to the ordering temperature of 6 K and therefore we can assume that the magnetic ordering only takes place within the  $\Gamma_8^{(1)}$  quartet.

The wave functions  $|\tilde{m}\rangle$  of this quartet are linear combinations of the  $|m_z\rangle$  and are given by Lea et al. [25]. The coefficients are functions of the crystal field parameter  $x$ . We take  $x = 0.8$  close to the value calculated within the approximation of the point charge model,  $x = 0.836$  [8].

The susceptibility  $\chi$  is anisotropic in such a quartet, depending on the direction of the applied field with respect to the crystal lattice. As the magnetic field is perpendicular to the  $[111]$  axis and is randomly oriented inside the crystallite  $(111)$  plane, the susceptibility tensor  $\bar{\chi}$  is isotropic in this plane and on average  $\bar{\chi} = \chi_{zz}$ .

In the limit of low applied fields, the Zeeman effect can be considered as a perturbation of the crystal field level and

we limit the calculation to the first order perturbation Zeeman term linear in  $H$ .

$$\chi = \frac{\mu_0 N}{\Psi} \sum_{n,m} \left[ \frac{|\langle \tilde{m} | \mu_z | \tilde{m} \rangle|^2}{k_B T} \exp(-E_n/k_B T) \right] \quad (1)$$

with  $\Psi = \sum_n \exp(-E_n/k_B T)$ , and where  $N$  is the atom density,  $E_n$  is the energy of the crystal field level  $\Gamma_n$  and  $\mu_z = g \mu_B m_z$ . As  $E[\Gamma_8^{(2)} - \Gamma_8^{(1)}] \approx 90$  K, we neglect the contribution of the upper  $\Gamma_8^{(2)}$  quartet and all upper levels and calculate the summation in the ground state. In the approach of a Curie-Weiss variation, that is, at low applied field and temperatures higher than  $T_C$ ,  $\chi = C/(T - \theta_p)$ , we therefore obtain inside the  $\Gamma_8^{(1)}$  quartet:

$$C = \frac{\mu_0 N g_J^2 \mu_B^2}{k_B} \sum_{\Gamma_8} \left[ \frac{1}{4} |\langle \tilde{m} | \mu_z | \tilde{m} \rangle|^2 \right]. \quad (2)$$

Finally the calculated effective moment within this approach is:  $\mu_{\text{eff}} = 7.95 \mu_B$ , in agreement with the measured low temperature effective moment  $\mu_{\text{eff}} = 7.56 \pm 0.1 \mu_B$ .

#### 4. Conclusion

Highly stoichiometric ErN nanocrystalline films have been grown on a silicon substrate, passivated with a GaN capping layer and found to be semiconductors. These films are ferromagnetic below a Curie temperature of 6 K. The magnetic ordering takes place inside a crystal field quartet ground state. The low temperature susceptibility agrees with the theoretical value calculated within a simple point charge model. Furthermore, the extrapolated spontaneous magnetization at 2 K can be quite well explained in the magnetic structure model proposed for HoN by neutron diffraction [13] with the moments along  $\langle 001 \rangle$  directions, arranged in successive ferromagnetic  $(111)$  planes. Such a structure shows a better agreement than the up-to-now accepted assumption of easy axes perpendicular to  $[111]$ .

#### Acknowledgments

The authors are grateful to J. Kennedy for the RBS/NRA measurements. The MacDiarmid Institute is supported by the New Zealand Centres of Research Excellence Fund and the research reported here by a grant from the New Zealand New Economy Research Fund. C.M. is grateful to the staff of the School of Chemical and Physical Sciences for their hospitality, and acknowledges the financial support of the MacDiarmid Institute and of the Royal Society of New Zealand.

#### References

- [1] C.-G. Duan, R.F. Sabirianov, W.N. Mei, P.A. Dowben, S.S. Jaswal, E.Y. Tsymlal, J. Phys. Condens. Matter 19 (2007) 315220.
- [2] C.M. Aerts, P. Strange, M. Horne, W.M. Temmerman, Z. Szotek, A. Svane, Phys. Rev. B 69 (2004) 045115.
- [3] S. Granville, B.J. Ruck, F. Budde, A. Koo, D.J. Pringle, F. Kuchler, A.R.H. Preston, D.H. Housden, N. Lund, A. Bittar, G.V.M. Williams, H.J. Trodahl, Phys. Rev. B 73 (2006) 235335.
- [4] H.J. Trodahl, A.R.H. Preston, J. Zhong, B.J. Ruck, N.M. Strickland, C. Mitra, W.R.L. Lambrecht, Phys. Rev. B 76 (2007) 085211.
- [5] A.R.H. Preston, S. Granville, D.H. Housden, B. Ludbrook, B.J. Ruck, H.J. Trodahl, A. Bittar, G.V.M. Williams, J.E. Downes, K.E. Smith, W.R.L. Lambrecht, Phys. Rev. B 76 (2007) 245120.
- [6] C. Meyer, B.J. Ruck, J. Zhong, S. Granville, A.R.H. Preston, G.V.M. Williams, H.J. Trodahl, Phys. Rev. B 78 (2008) 174406.
- [7] P. Larson, W.R.L. Lambrecht, A. Chantis, M. van Schilfgarde, Phys. Rev. B 75 (2007) 045114.
- [8] F. Hulliger, Handbook on the Physics and Chemistry of Rare Earths, vol. 4, North-Holland Physics Publishing, New York, 1978, pp. 153–236.
- [9] O. Vogt, K. Mattenberger, Handbook on the Physics and Chemistry of Rare Earths, vol. 17, Elsevier, Amsterdam, 1993, pp. 301–407.

- [10] G. Busch, P. Junod, F. Levy, A. Menth, O. Vogt, Phys. Lett. 14 (1965) 264.
- [11] G. Busch, J. Appl. Phys. 38 (1967) 1386.
- [12] G.L. Olcese, J. Phys. F 9 (1979) 569.
- [13] H.R. Child, M.K. Wilkinson, J.W. Cable, W.C. Koehler, E.O. Wollan, Phys. Rev. 131 (1963) 922.
- [14] O. Vogt, K. Mattenberger, J. Alloys Compd. 223 (1995) 226.
- [15] N. Sclar, J. Appl. Phys. 35 (1964) 1534.
- [16] S. Sanna, B. Hourahine, U. Gerstmann, Th. Frauenheim, Phys. Rev. B 76 (2007) 155128.
- [17] C.-G. Duan, R.F. Sabirianov, J. Liu, W.N. Mei, P.A. Dowben, J.R. Hardy, J. Appl. Phys. 97 (2005) 10A915.
- [18] G.T. Trammell, Phys. Rev. 131 (1963) 932.
- [19] S.J. Allen Jr., N. Tabatabaie, C.J. Palmstrøm, G.W. Hull, T. Sands, F. DeRosa, H.L. Gilchrist, K.C. Garrison, Phys. Rev. Lett. 62 (1989) 2309.
- [20] T. Nakagawa, T. Arakawa, K. Sako, N. Tomioka, T.A. Yamamoto, T. Kusunose, K. Niihara, K. Kamiya, T. Numazawa, J. Alloys Compd. 408–412 (2006) 191.
- [21] R.J. Gambino, T.R. McGuire, H.A. Alperin, S.J. Pickart, J. Appl. Phys. 41 (1970) 933.
- [22] R.A. Cutler, A.W. Lawson, J. Appl. Phys. 46 (1975) 2739.
- [23] S. Granville, Ph.D. Thesis, University of Wellington, 2006.
- [24] J. Schneider, H.D. Müller, J.D. Ralston, F. Fuchs, A. Dörnen, K. Thonke, Appl. Phys. Lett. 59 (1991) 34.
- [25] K.R. Lea, M.J.M. Leask, W.P. Wolf, J. Phys. Chem. Solids 23 (1962) 1381.